Journal of Alloys and Compounds 369 (2004) 152–154

Journal of ALLOYS AND COMPOUNDS

www.elsevier.com/locate/jallcom

Enhanced magnetic properties in Zr-containing rare earth-rich Didymium (Nd/Pr)-based nanocrystalline hard magnetic alloys

I. Betancourt [a,*], H.A. Davies [b]

[a] *Materials Research Institute, UNAM, P.O. Box 70-360, Mexico, DF 04510, Mexico*
[b] *Department of Engineering Materials, University of Sheffield, Sheffield S13JD, UK*

Abstract

A systematic study of the influence of processing conditions and Zr addition on the magnetic properties of RE-rich, Didymium $(Nd/Pr)_{14}Fe_{80}B_6$ (Nd:Pr ratio of 3:1) is reported. For directly quenched alloys, various roll speeds resulted in grain sizes d_g within the range 35–50 nm. Increasing remanence J_r and maximum energy product $(BH)_{max}$ values were observed as d_g decreased (up to 0.86 T and up to 124 kJ/m^3, respectively). Small Zr addition (1 at.%) resulted in improved J_r and $(BH)_{max}$ (up to 0.92 T and up to 142 kJ/m^3, respectively). For overquenched and annealed alloys, partial substitution of Fe by Zr (0–4 at.%) indicated a marked dependence of the magnetic properties on Zr content, with an excellent combination of J_r, (1.0 T), $_iH_c$ (1574 kA/m) and $(BH)_{max}$ (149 kJ/m^3) at 2 at.% Zr. Results are interpreted in terms of variations in the scale of the nanostructure and of the effects of Zr substitutions into the 2/14/1 unit cell.

Keywords: Permanent magnets; Magnetic measurements

1. Introduction

The processing windows for obtaining optimum nanostructures and magnetic properties by direct quenching via melt spinning to ribbons in NdFeB-based alloys tend to be narrow and the properties within large batches are likely to be rather variable [1]. An alternative process route is to overquench to a fully amorphous state, followed by a controlled devitrification anneal to a nanoscale grain structure. This has been shown, in some cases, to yield magnetic properties comparable with those attainable by direct quenching [2]. Also, the substitution of Nd by Pr in nanostructured $RE_2Fe_{14}B$ hard magnetic alloys is of interest because the anisotropy field H_A and the intrinsic coercivity $_iH_c$, are increased [3]. For RE-rich compositions ($y > 12$ in $RE_yFe_{94-y}B_6$ alloy systems) having already large $_iH_c$ values (typically above 1000 kA/m) this substitution is expected to increase $_iH_c$ values for similar processing conditions [3]. Moreover, Zr additions in stoichiometric $RE_2Fe_{14}B$ alloys have been reported as increasing the anisotropy field H_A, since Zr enters the $RE_2Fe_{14}B$ unit cell [4–6].

In this paper, the effect of processing conditions and Zr addition on the magnetic properties of RE-rich, Didymium $(Nd/Pr)_{14}Fe_{80}B_6$ (Nd:Pr ratio of 3:1) alloys, produced by direct quenching and by overquenching and annealing, is presented.

2. Experimental techniques

Ingots of the alloys were prepared using commercial grade materials by arc-melting the constituents in a high purity Ar atmosphere. The compositions of the alloys were $(Nd_{0.75}Pr_{0.25})_{14}Fe_{80-x}Zr_xB_6$ ($x = 0$–4). Nanocrystalline directly quenched (DQ) ribbon samples with thicknesses and mean grain sizes in the range 20–40 μm and 35–50 nm, respectively, were produced by chill block melt spinning at various roll speeds (16–25 m/s), under a protective argon atmosphere. Overquenched and annealed alloys (OA) were obtained by devitrification of fully amorphous alloy spun at 45 m/s (annealed 10 min at 700 °C with material sealed in a silica tube under argon). The magnetic properties J_r, $_iH_c$ and $(BH)_{max}$ (computed from the BH loop) were determined using an Oxford Vibrating Sample Magnetometer with a maximum field of 5 T. Measurements were made in the

* Corresponding author. Fax: +52-55-56161-371.
E-mail address: israelb@correo.unam.mx (I. Betancourt).

0925-8388/$ – see front matter © 2003 Published by Elsevier B.V.
doi:10.1016/j.jallcom.2003.09.090

plane of the ribbon samples and transverse to the spinning direction so that no correction for self-demagnetisation was necessary. The Curie temperature T_c of the 2/14/1 phase was determined by DSC, using a heating rate of 40 K/min. The structures of selected ribbon samples were monitored by X-ray diffractometry and the mean crystallite diameter d_g for the 2/14/1 phase was estimated by line broadening analysis, using the Scherrer formula [7].

3. Results and discussion

XRD diffractograms for nanocrystalline $(Nd_{0.75}Pr_{0.25})_{14}Fe_{80}B_6$ alloys, melt spun at various roll speeds v_r, are shown in Fig. 1. For increasing v_r, a slight broadening of the peaks is manifested, which results in decreasing d_g values. Also included in Fig. 1 is the diffractogram of a Zr-containing sample, which exhibits a further peak broadening as a consequence of an additional grain size refinement. The effects of varying d_g on the magnetic properties of DQ $(Nd_{0.75}Pr_{0.25})_{14}Fe_{80}B_6$ alloys are plotted in Fig. 2. J_r increases progressively rapidly as d_g decreases up to 0.86 ± 0.03 T for $d_g = 36$ nm, reflecting the increasing degree of intergranular exchange coupling. The magnitude of J_r for any given d_g is lower than for the lower RE-containing ($\leq$12 at.%) alloys because of the dilution of the 2/14/1 phase by the paramagnetic RE-rich grain boundary phase [8]. $(BH)_{max}$ follows the same trend, as is expected for alloys in which ${}_iH_c \geq J_r/2$ [9], up to 124 ± 3 kJ/m^3 at $d_g = 36$ nm. Unlike stoichiometric alloys [8], ${}_iH_c$ also increases as d_g decreases, up to a maximum of 1500 ± 30 kA/m at $d_g = 38$ nm. Such high ${}_iH_c$ can be ascribed to the significant role of grain boundary phase in damping the nucleation of reverse domains. This grain boundary effect is likely to be strengthened as d_g decreases due to increased boundary area per unit volume, though it may be in competition with the effect of increasing exchange coupling in decreasing ${}_iH_c$. Such a competition may explain why ${}_iH_c$ manifests a maximum value. Upon substituting 1 at.% Zr for Fe, a significant refinement of d_g down to 28 nm was observed for samples melt spun at 25 m/s. This resulted in increased remanence enhancement up to 0.92 ± 0.01 T and, thus, in an improved $(BH)_{max}$ of 142 ± 2 kJ/m^3, with only a small attenuation of ${}_iH_c$ (1322 ± 20 kA/m). These represent an excellent combination of magnetic properties.

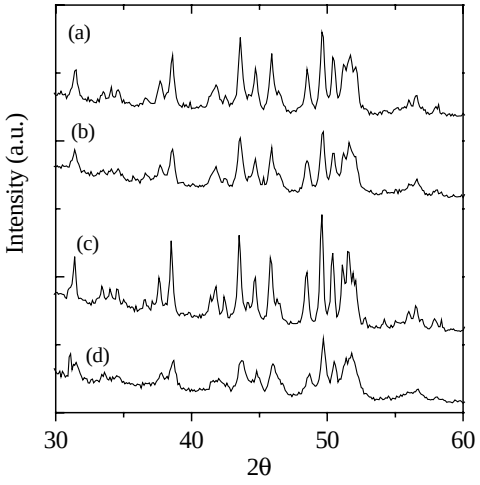

Fig. 1. XRD diffractograms for nanocrystalline DQ $(Nd_{0.75}Pr_{0.25})_{14}Fe_{80}B_6$ alloys, melt spun at various v_r, showing d_g variations: (a) $v_r = 18$ m/s, $d_g = 42$ nm; (b) $v_r = 22$ m/s, $d_g = 39$ nm; (c) $v_r = 25$ m/s, $d_g = 36$ nm; (d) $v_r = 25$ m/s, 1 at.% Zr, $d_g = 28$ nm.

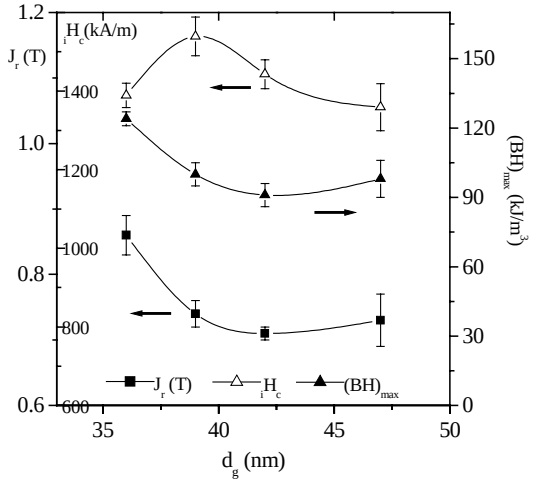

Fig. 2. Magnetic properties of $(Nd_{0.75}Pr_{0.25})_{14}Fe_{80}B_6$ DQ alloys as a function of d_g.

The mean grain size diameter d_g of the 2/14/1 phase as a function of Zr concentration for OA $(Nd_{0.75}Pr_{0.25})_{14}Fe_{80-x}Zr_xB_6$ (x = 0–4) alloy ribbons are shown in Fig. 3. Unlike the 0 and 1 at.% Zr DQ ribbons, the initial Zr addition (1 at.%) gave an increased d_g, though further Zr substitutions led to reduction of d_g. The magnetic properties as a function of Zr content are shown in Fig. 4. For the Zr-free OA alloy, an enhanced J_r of 0.84 ± 0.03 T, compared with

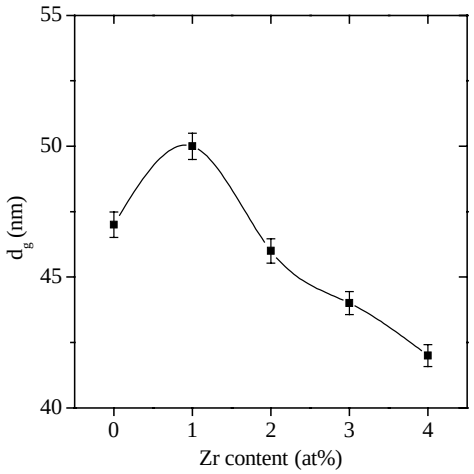

Fig. 3. Mean grain size diameter of the 2/14/1 phase as a function of Zr concentration for OA $(Nd_{0.75}Pr_{0.25})_{14}Fe_{80-x}Zr_xB_6$ (x = 0–4) alloy ribbons.

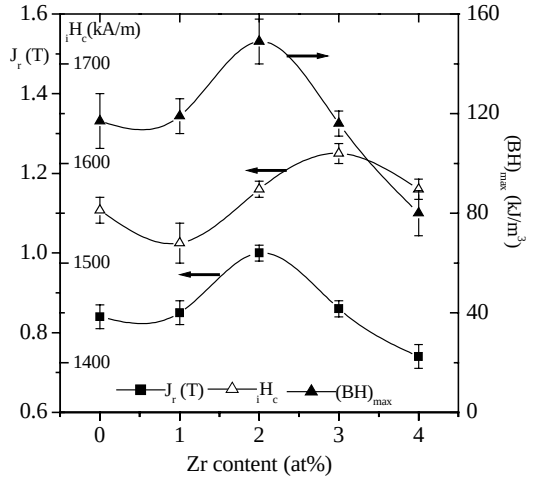

Fig. 4. Dependence of magnetic properties on Zr content for OA $(Nd_{0.75}Pr_{0.25})_{14}Fe_{80-x}Zr_xB_6$ ($x = 0$–4) alloy ribbons.

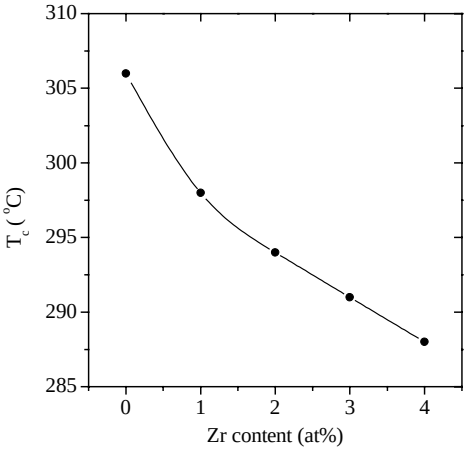

Fig. 5. T_c of the 2/14/1 phase, as a function of Zr concentration for OA $(Nd_{0.75}Pr_{0.25})_{14}Fe_{80-x}Zr_xB_6$ ($x = 0$–4) alloy ribbons.

the DQ counterpart with a $(BH)_{max}$ of 117 ± 11 kJ/m^3 were attained, for an equivalent d_g of 47 nm. $_iH_c$, in contrast, is very high (1553 ± 15 kA/m) and is about 12% larger than for the DQ equivalent. For Zr-containing samples, the initial Zr addition (1 at.%) gave little significant change in J_r (from 0.84 to 0.85 T), whilst, at 2 at.% Zr, a clear maximum ($J_r = 1.00 \pm 0.02$ T) was observed, presumably because of the reduced d_g promoting increased intergranular exchange interaction. Further increase in Zr concentration results in decreasing J_r, in spite of concomitant reduced d_g, evidently because of a diminishing saturation polarization J_s. As expected, $(BH)_{max}$ follows the same trend as J_r (since $(BH)_{max}$ is dominated by J_r at this level of $_iH_c$) with a maximum of 149 ± 9 kJ/m^3 at 2 at.% Zr. Overall, up to 3 at.% addition of Zr results in an increase in $_iH_c$, in spite of the decreasing d_g, which is consistent with an enhancement of H_A for the 2/14/1 phase [4], though initially, up to 1 at.% Zr, there is a slight decrease of $_iH_c$, presumably due to the increased d_g. The maximum $_iH_c$ at 3 at.% Zr is 1610 ± 10 kA/m. However, the best $(BH)_{max}/_iH_c$ combination (149 kJ/m^3/1574 kA/m) correspond to the 2 at.% Zr alloy, which are outstanding properties and exceed those of the 1 at.% Zr DQ sample, referred to above. The Curie temperature T_c of the 2/14/1 phase as a function of Zr concentration is shown in Fig. 5. For the Zr-free sample, a slightly reduced T_c (306 °C) compared with the $Nd_2Fe_{14}B$ phase (310 °C) is observed as a consequence of the partial substitution of Nd by Pr. A monotonic decrease of T_c with increasing Zr content is observed, which we conclude is evidence for the Zr entering into the $RE_2Fe_{14}B$ unit cell, and influencing the inter-atomic exchange interactions. Thus, for the alloy having the most favourable $(BH)_{max}/_iH_c$ combination (2 at.% Zr) the reduction in T_c is ~12 °C. This could be compensated for by small substitution of Co for Fe.

4. Conclusions

Excellent combinations of coercivity and maximum energy product have been achieved for nanocrystalline mixed rare earth melt spun $(Nd_{0.75}Pr_{0.25})_{14}Fe_{80}B_6$-based alloys through small substitutions of Zr for Fe. For directly quenched $(Nd_{0.75}Pr_{0.25})_{14}Fe_{79}Zr_1B_6$ the $(BH)_{max}$ and $_iH_c$ were 142 kJ/m^3 and 1322 kA/m, respectively, while, for the overquenched and annealed (700 °C for 10 min) $(Nd_{0.75}Pr_{0.25})_{14}Fe_{78}Zr_2B_6$ ribbon, the values were 149 kJ/m^3 and 1574 kA/m, respectively.

Acknowledgements

H.A. Davies acknowledges financial support from EPSRC, through the Advanced Magnetics Programme.

References

[1] H.A. Davies, in: C.F. Mainwaring, et al. (Eds.), Proceedings of the 8th Symposium on Magnetic Anisotropy and Coercivity in RE-TM Alloys, University of Birmingham UK, 1994, p. 465.
[2] D. Goll, H. Kronmuller, in: L. Schultz, K.H. Muller (Eds.), Proceedings of the 15th International Workshop on RE Magnets and their Applications, MATINFO Frankfurt, 1998, p. 189.
[3] I. Betancourt, H.A. Davies, J. Appl. Phys. 85 (1999) 5911.
[4] M. Jurczyk, W.E. Wallace, J. Magn. Magn. Mater. 59 (1986) L182.
[5] T.W. Capehart, R.K. Mishra, F.E. Pinkerton, J. Appl. Phys. 73 (1993) 6476.
[6] J.I. Betancourt, H.A. Davies, IEEE Trans. Magn. 37 (2001) 2480.
[7] G.E. Carr, H.A. Davies, R.A. Buckley, Mater. Sci. Eng. 99 (1988) 147.
[8] H.A. Davies, J. Magn. Magn. Mater. 157–158 (1996) 11.
[9] D. Goll, M. Seeger, H. Kronmuller, J. Magn. Magn. Mater. 185 (1998) 49.